AMERICAN JOURNAL OF PHYSIOLOGY
HEART AND CIRCULATORY PHYSIOLOGY

Am J Physiol Heart Circ Physiol 327: H967–H977, 2024.
First published September 6, 2024; doi:10.1152/ajpheart.00646.2023

RESEARCH ARTICLE

Cardiovascular Complications of Pregnancy

Gestational influenza A virus infection elicits nonresolving vascular dysfunction and T-cell accumulation in the aorta of mice

Osezua Oseghale,[1] Kylie M. Quinn,[1,2] Madison Coward-Smith,[1] Felicia Liong,[1] Mark A. Miles,[1] Robert D. Brooks,[3] Ross Vlahos,[1] John J. O'Leary,[4,5,6] Doug A. Brooks,[3] Stella Liong,[1]* and Stavros Selemidis[1]*

[1]*School of Health and Biomedical Sciences, RMIT University, Melbourne, Victoria, Australia;* [2]*Department of Biochemistry, Biomedicine Discovery Institute, Monash University, Melbourne, Victoria, Australia;* [3]*Clinical and Health Sciences, University of South Australia, Adelaide, South Australia, Australia;* [4]*Discipline of Histopathology, School of Medicine, Trinity Translational Medicine Institute, Trinity College Dublin, Ireland;* [5]*Sir Patrick Dun's Laboratory, Central Pathology Laboratory, St. James's Hospital, Dublin, Ireland; and* [6]*CERVIVA Research Consortium, Trinity College, Dublin, Ireland*

Abstract

T-cell accumulation within the aorta promotes endothelial dysfunction and the genesis of cardiovascular disease, including hypertension and atherosclerosis. Viral infection during pregnancy is also known to mediate marked acute endothelial dysfunction, but it is not clear whether T cells are recruited to the aorta and whether the dysfunction persists postpartum. Here, we demonstrate that influenza A virus (IAV) infection during pregnancy in a murine model resulted in endothelial dysfunction of the aorta, which persisted for up to 60 days postinfection and was associated with higher levels of IFN-γ mRNA expression within the tissue. In the absence of infection, low numbers of naïve $CD4^+$ and $CD8^+$ T cells, central memory T cells, and effector memory T cells were observed in the aorta. However, with IAV infection, these T-cell subsets were significantly increased with a notable accumulation of IAV-specific $CD8^+$ effector memory T cells. Critically, this increase was maintained out to at least 60 days. In contrast, IAV infection in nonpregnant female mice resulted in modest endothelial dysfunction with no accumulation of T cells within the aorta. These data, therefore, demonstrate that the aorta is a site of T-cell recruitment and retention after IAV infection during pregnancy. Although IAV-specific memory T cells could theoretically confer protection against future influenza infection, nonspecific memory T-cell activation and IFN-γ production in the aorta could also contribute to future endothelial dysfunction and cardiovascular disease.

NEW & NOTEWORTHY Pregnancy is a risk factor for cardiovascular complications to influenza A virus (IAV) infection. We demonstrate that gestational IAV infection caused endothelial dysfunction of the maternal aorta, which persisted for 60 days postinfection in mice. Various T cells accumulated within the aorta at 60 days because of the infection, and this was associated with elevated levels of the proinflammatory cytokine, IFN-γ. Our study demonstrates a novel "long influenza" cardiovascular phenotype in female mice.

influenza; memory T cells; pregnancy; vascular dysfunction

INTRODUCTION

Influenza A virus (IAV) infection during pregnancy is associated with significantly higher morbidity and mortality in women (1). During seasonal influenza epidemics, pregnant women are five times more likely to be hospitalized and three to four times more predisposed to cardiopulmonary events (2, 3). In addition, the risk of IAV-induced respiratory complications increases with underlying comorbidities, such as hypertension (4). Pregnant women undergo immunological and physiological adaptations that are essential in modulating the maternal immune system to prevent fetal rejection and to facilitate oxygen and nutrient supply (5, 6). Our recent studies demonstrated that IAV infection during pregnancy in mice resulted in acute inflammation of the aorta and endothelial dysfunction, which we have termed the "vascular storm" (7). This is characterized by a profound innate and adaptive inflammatory immune response (6) with early infiltration of neutrophils and monocytes followed by a delayed accumulation of T cells within the aorta, which was associated with endothelial dysfunction.

Although the acute effects of the "vascular storm" triggered by IAV infection during pregnancy were previously characterized, little is known about the chronic impacts of endothelial

*S. Liong and S. Selemidis contributed equally to this work.
Correspondence: S. Liong (stella.liong@RMIT.edu.au); S. Selemidis (Stavros.selemidis@RMIT.edu.au).
Submitted 9 October 2023 / Revised 12 August 2024 / Accepted 28 August 2024

dysfunction and immune cell recruitment in pregnancy, specifically, whether T cells that accumulate during initial infection are retained in the tissue or whether these cells impact on aortic function at later time points. T cells are known to play a critical role in the development and progression of hypertension more generally. Indeed, Guzik et al. (8) demonstrated that T cells play an important role in angiotensin II-induced hypertension. The aortic T-cell activation profile observed in hypertensive mouse models is comparable to the phenotype observed during IAV infection in pregnancy (9). Given that T-cell accumulation is observed in both hypertension and IAV infection during pregnancy, we hypothesize that this may establish persistent memory T-cell populations within the aorta.

Memory T cells are distinct from naïve T cells in that they become activated by a lower antigen density and more quickly upon interaction with their target antigen (10–12). Memory T cells can also be more sensitive to cytokines, which can result in antigen-independent or "bystander" activation of T-cell functions (13). The adhesion molecules CD44 and CD62L are used to delineate key subsets within $CD4^+$ and $CD8^+$ T-cell populations, including $CD44^-CD62L^+$ naïve T cells, $CD44^+CD62L^+$ central memory T cell (T_{CM}) and $CD44^+CD62L^-$ effector memory T cell (T_{EM}; 14). Of note, resident memory T (T_{RM}) cells have been characterized more recently, which are memory cells that reside long term within tissues. T_{RM} cells are $CD44^{hi}CD69^{hi}$ and can coexpress CD103 in certain tissues based on local transforming growth factor-β availability (15). T_{EM} and T_{RM} cells can secrete high levels of IFN-γ to clear pathogens and drive endothelial and vascular smooth muscle cell (VSMC) apoptosis, contributing to endothelial dysfunction (16, 17). Indeed, T_{EM} cells are suggested to exacerbate hypertension when repeated hypertensive or inflammatory stimuli are introduced (18). Accordingly, IAV infection during pregnancy could result in the recruitment of T_{EM} and/or T_{RM} cells into the aorta, which are able to persist, rapidly secrete cytokines, and contribute to long-term vascular pathogenesis.

Our findings illustrate that IAV infection during pregnancy results in prolonged vascular endothelial dysfunction up to at least *day 60* after infection, which is associated with elevated expression of IFN-γ mRNA in the aortic tissue. In parallel, we saw a persistent increase in both naive and memory $CD8^+$ and $CD4^+$ T cells within the aortic tissue for at least 60 days after infection, most notably of IAV-specific cells and cells expressing activation markers. This evidence supports our model that IAV infection during pregnancy establishes memory T-cell populations in the aorta capable of generating IFN-γ and mediating chronic vascular dysfunction, which defines an important long-influenza phenotype within the cardiovascular system.

MATERIALS AND METHODS

Mice, Virus, and Infection

Nonpregnant and pregnant (8–12 wk) C57BL6/J mice were obtained from the Animal Resources Center, Western Australia, Australia, and maintained in a 12-h:12-h light/dark cycle with food and water at the animal research facility (RMIT University, Bundoora, Australia). All experiments were conducted according to approval obtained from the Animal Experimentation Ethics Committee of the Royal Melbourne Institute of Technology University (RMIT) Animal Ethics Committee (Ethics No. 1801) and in compliance with the guidelines of the National Health and Medical Research Council (NHMRC) of Australia on animal experimentation. Mice were lightly sedated with isoflurane inhalation and infected intranasally at *embryonic day 12* (E12) gestation with 10^4 plaque-forming units of recombinant HK-x31 (H3N2) mouse-adapted influenza A virus strain or phosphate-buffered saline (PBS, Sigma) for controls and followed for 12-, 30-, and 60-days postinfection (dpi).

Blood Pressure Measurements

Tail cuff plethysmography using the BP-2000 Series II Blood Pressure Analysis System (Visitech Systems) was performed on restrained conscious mice. Mice were acclimatized for at least 4 consecutive days before recording blood pressure measurements at either 6 or 60 dpi. Recordings were taken from 20 individual measurements for systolic pressure. Values that were greater than two standard deviations from the mean value were considered outliers and excluded from the final analysis.

Vascular Reactivity

Aortic vascular function was determined by myography, as previously described (7, 9). Briefly, thoracic aortic rings were harvested and dissected free of perivascular adipose tissue from 12 ($n = 5$ PBS; $n = 4$ HK-x31)-, 30 ($n = 8$ PBS; $n = 7$ HK-x31)-, and 60 ($n = 6$ PBS; $n = 11$ HK-x31)-dpi pregnant mice and 60-dpi nonpregnant female mice ($n = 6$ PBS; $n = 6$ HK-x31). Thoracic aortae were cut into 2 mm rings and mounted onto two stainless steel pins on a four-channel wire myograph (Danish Myo Technology, Hinnerup, Denmark). Vessels were stimulated with a final concentration of 1×10^{-6} M of thromboxane A2 receptor agonist U46619 (Cayman, Michigan) to determine smooth muscle-dependent contraction (19). Endothelium- and nitric oxide-dependent relaxation was assessed using increasing concentrations (1×10^{-9} M–1×10^{-5} M) of acetylcholine (ACh) in the aorta, which were precontracted to 50% of their U46619 contraction with U46619. Also, in some rings of the aorta, the endothelium-independent vascular smooth muscle relaxation response to the nitric oxide donor, sodium nitroprusside (SNP; 1×10^{-9} M–1×10^{-5} M) was examined.

Major Histocompatibility Complex Class I-Peptide Tetramer

Major histocompatibility complex (MHC) class I-peptide tetramer was generated by the Innate Immunity and Anti-Viral Immunity Laboratory in the Department of Microbiology and Immunology, University of Melbourne. The tetramer used in this study (MHC class I $D^bPA_{224}{}^+$) has been shown to be highly specific for $CD8^+$ T cells (20, 21).

Flow Cytometry

Maternal thoracic aortae harvested at 30 and 60 dpi were flushed with PBS to rid the vessel of excess blood. Aortae were processed into a single cell suspension for flow cytometry analysis, as previously described (7, 9). Briefly, aortae

were mechanically minced and digested in digestion buffer [0.156 mg/mL Collagenase type XI (Cat. No. C7657, Sigma), 0.03 mg/mL hyaluronidase (Cat. No. H3884, Sigma), and 1.8 mg/mL Collagenase Type I-S (Cat. No. C1639, Sigma)] for 1 h at 37°C. Cell suspensions were filtered through a 70-μm strainer and washed twice with FACS buffer (PBS containing 2.5% FBS). Cells were then stained for 15 min at 4°C with the following antibodies: 1:200 anti-CD45 (30-F11); 1:200 anti-CD8 (53-6.7); 1:200 anti-CD4 (RM4-5); 1:200 anti-CD69 (H1.2F3); 1:200 anti-CD44 (IM7); 1:200 anti-CD62L (MEL-14) and 1:1,000 live/dead fixable aqua dead cell stain kit (Invitrogen). Following immunostaining, cells were analyzed on the BD LSRFortessa X-20 flow cytometry analyzer with DIVA software (Becton Dickinson Bioscience). Data were analyzed using FlowJo software (Tree Star). The cells were analyzed as a percentage of live $CD45^+$ or $CD8^+$ cells or expressed in absolute numbers per 25,000 counting beads.

Quantification of mRNA by QPCR

Maternal lung and thoracic aorta were harvested from pregnant mice on 30 and 60 dpi for RNA extraction using the RNeasy Mini kit (Cat. No. 74104, Qiagen), as per manufacturer's instructions. cDNA was then synthesized from 1.0 to 2.0 μg of total RNA using the High-Capacity cDNA Reverse Transcription Kit (Applied Biosystems, Foster City, CA). Total RNA was added to a Master Mix mixture of reagents in the High-Capacity cDNA RT kit, as previously described (7, 9). QPCR was then performed using the TaqMan Universal PCR Master Mix (Applied Biosystems, Foster City, CA) and analyzed on the Applied biosystem QuantStudio 7 Flex Real-Time PCR System (Thermo Fisher Scientific, Waltham, MA). IFN-γ and IAV polymerase primers were included in the Assay on-Demand Gene Expression Assay Mix (Applied Biosystems, Foster City, CA). The quantitative values were obtained from the threshold cycle (Ct) number. Gene expression analysis was performed using the comparative Ct method. Each individual target gene expression was normalized against RPS18 mRNA expression and expressed relative to the control.

Statistical Analysis

All data were expressed as means ± SE. All comparisons between experimental groups, unless specified otherwise, were performed by unpaired *t* test or a Mann–Whitney test if data were not normally distributed. Dose-response curve analysis for vascular reactivity studies was performed using a two-way ANOVA for repeated measures with either Tukey's or Holm's Sidak multiple comparison test. E_{max} and EC_{50} values could not be determined as dose-response curves were not sigmoidal, and area under the curve (AUC) analysis was performed instead. Statistical tests were performed using GraphPad Prism (GraphPad Software v.8.2, San Diego, CA). Statistical significance was considered at $P < 0.05$.

RESULTS

IAV Infection Induces Vascular Dysfunction That Persists in the Maternal Thoracic Aorta

To examine the long-term effect of IAV infection on vascular function, we performed a series of experiments using wire myography to analyze the functionality of the aorta post-viral clearance. Pregnancy outcomes found no differences in gestation at delivery nor with litter sizes; however, there were increased pup deaths following IAV infection (Supplemental Fig. S2; Supplemental figures can be accessed at https://doi.org/10.25439/rmt.26156272). IAV infection in E12.5 pregnant mice resulted in an impairment in the response to endothelial-dependent vasodilator ACh at 12 dpi (Fig. 1, *A* and *B*) but no significant impairment was observed in the response to the endothelial-independent vasodilator SNP (Fig. 1*C*), which corroborates with our previous observations following IAV infection at 6 dpi (7). The impairment in endothelium-dependent relaxation to ACh persisted in the aorta at 30 dpi (~60% relaxation compared with 80% in the uninfected controls; Fig. 1*D*) and at 60 dpi (~40% relaxation compared with 80% in the uninfected controls; Fig. 1*F*). In contrast, endothelium-independent relaxation to SNP in IAV-infected pregnant mice was comparable to uninfected controls at 30 dpi (Fig. 1*E*) and 60 dpi (Fig. 1*G*). We also assessed endothelial-dependent relaxation of the aorta of nonpregnant mice infected with IAV at 60 dpi (Fig. 1*H*). Endothelial dysfunction was only modest, showing a slight rightward shift but no change in the maximal relaxation response. Area-under-the-curve (AUC) analysis was also performed, which showed similar results to the dose-response curves (Supplemental Fig. S3). In addition, a constriction response to U46619 showed no change at 12 and 30 dpi (Fig. 2, *A* and *B*). The aortic constriction response to U46619 at 60 dpi, however, was significantly reduced in IAV-infected pregnant mice, whereas there was no change with IAV-infected nonpregnant mice at the same time point (Fig. 2, *C* and *D*). These findings suggest that the IAV-induced long-term vascular dysfunction is profound when the infection occurs during pregnancy with evidence of significant endothelial and vascular smooth muscle dysfunction, given the impairment in U46619-induced constriction. To determine if endothelial dysfunction was associated with hypertension, systolic blood pressure was also recorded at 6 dpi (during pregnancy) and 60 dpi (postpartum; Fig. 1*I*). We found a transient decrease in systolic blood pressure at *day 6*, which returned to uninfected levels at *day 60* after infection.

Given that IFN-γ is known to be associated with vascular dysfunction, we then used real-time PCR to measure the amount of IFN-γ transcript within aortic tissue. We found that there was a significant increase in IFN-γ mRNA expression at *day 30*, and this was maintained at *day 60* after infection (Fig. 1*J*). This suggests that a cell type within the aortic tissue is expressing IFN-γ mRNA up to 60 dpi.

IAV Infection Establishes a Persistent Population of $CD4^+$ and $CD8^+$ T Cells in the Aorta Post-Viral Clearance

We have previously shown that at 6 dpi, there was an accumulation of activated $CD8^+$ and $CD4^+$ T cells in the aorta (7). Given that vascular dysfunction persists beyond this time point despite the virus having been cleared, we aimed to determine whether there were persistent populations of $CD4^+$ and $CD8^+$ T cells in the aorta at 30 and 60 dpi. Indeed, the absolute number of both $CD4^+$ and $CD8^+$ T-cell populations was elevated at both 30 and 60 dpi (Fig. 3, *A–C*). The proportions of $CD4^+$ T cells were elevated at the 60-dpi time point with no differences observed at 30 dpi, while no

significant differences were observed with CD8$^+$ T-cell proportions (Fig. 3, *A*–*C*).

We next investigated whether the elevated population of CD8$^+$ T cells contained IAV-specific CD8$^+$ T cells in the aorta using an MHC class I tetramer loaded with the immunodominant PA_{224} peptide. In previous work, we have observed IAV dissemination and enhanced CD8$^+$ T-cell recruitment to the aorta at 3 and 6 dpi, respectively (7).

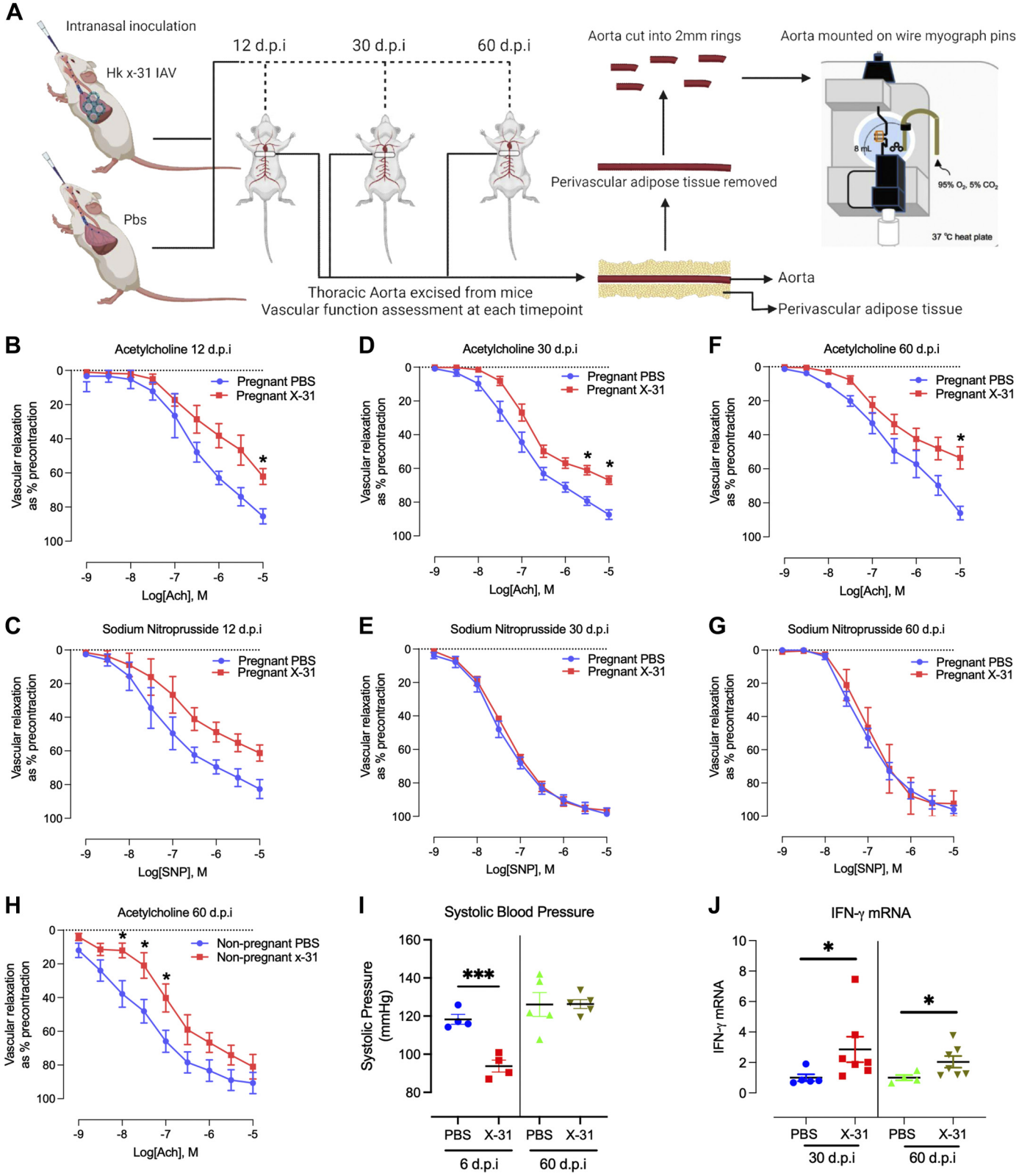

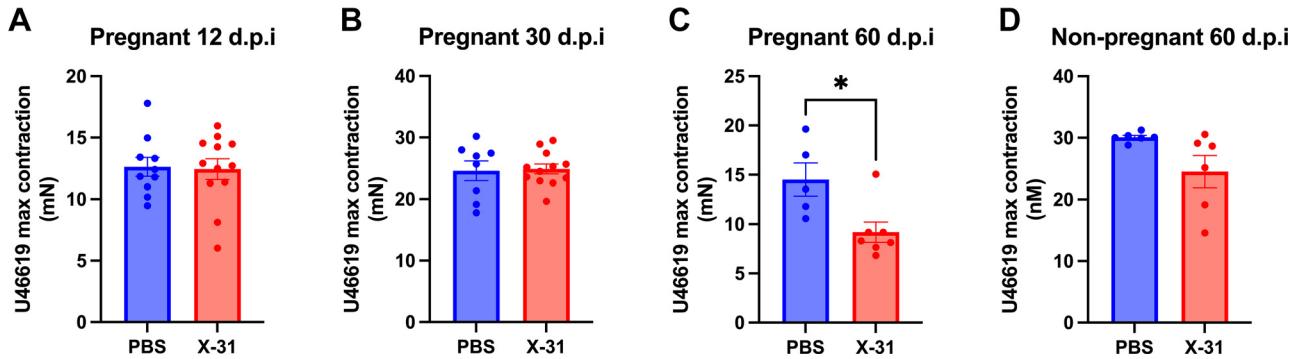

Figure 2. Aortic constriction response to thromboxane agonist U-46619 is impaired in influenza A virus X (IAV)-infected pregnant mice at 60 dpi. Vascular function was measured in isolated thoracic aortic rings of nonpregnant and pregnant mice infected with PBS or HKx-31 (x-31) at 10^4 pfu. *A–C*: aortic rings were isolated from pregnant mice at 12 (*A*), 30 (*B*), and 60 (*C*) dpi. *D*: aortic rings were also isolated from nonpregnant mice at 60 dpi. Maximal constriction force in response to thromboxane agonist U-46619 was then recorded. Data shown represent PBS, $n = 6–9$ animals; X-31, $n = 6–12$ animals; of at least two independent experiments. Results are presented as means ± SE. Unpaired Student's *t* test was used for statistical analysis against their respective PBS controls. pfu, plaque-forming units. $*P < 0.05$.

Consistent with this, we observed elevated proportions and in absolute numbers of IAV-specific $D^bPA_{224}{}^+$ $CD8^+$ T cell in the aorta at 30 and 60 dpi (Fig. 3, *D–F*).

IAV Infection Promotes Naïve and IAV-Specific Memory T-Cell Residence in the Aorta Post-Viral Clearance

We then aimed to determine whether $CD4^+$ and $CD8^+$ T cells in the aorta represent naïve or conventional memory T-cell subsets. Of note, both $CD4^+$ and $CD8^+$ T cells were predominantly $CD44^-CD62L^-$ in the aorta (Fig. 4, *A* and *B*), which is an unconventional T-cell population commonly seen within tissues. T_{EM} ($CD44^+CD62L^-$) $CD4^+$ and $CD8^+$ T cells were the major conventional memory T-cell population and were significantly elevated with IAV infection at both 30 and 60 dpi (Fig. 4, *A–D*). Naïve ($CD44^-CD62L^+$) and T_{CM} ($CD44^+CD62L^+$) $CD4^+$ and $CD8^+$ T-cell populations were more minor populations but were also elevated with IAV infection at 30 and/or 60 dpi (Fig. 4, *A–D*).

We then determined whether IAV-specific $CD8^+$ T cells in the aorta were derived from a specific memory T-cell subset. We observed that IAV-specific $CD8^+$ T cells predominantly exhibited a T_{EM} phenotype at both 30 and 60 dpi (Fig. 4, *E* and *F*) and T_{EM} phenotypic IAV-specific $CD8^+$ T cells were significantly elevated in number at both time points (Fig. 4*G*).

We explored whether $CD4^+$ and $CD8^+$ T cells in the aorta could include T_{RM} cells by measuring the coexpression of CD69 and CD44. We observed significantly elevated absolute numbers of T_{RM} phenotypic $CD4^+$ T cells at 60 dpi but not at 30 dpi (Fig. 5, *A* and *C*). Regarding the absolute numbers of T_{RM} phenotypic $CD8^+$ T cells, we observed a significant elevation at 30 dpi and a trend ($P = 0.07$) for an elevation at 60 dpi (Fig. 5, *B* and *D*). Finally, we examined T-cell populations in the aorta following IAV infection of nonpregnant mice. In striking contrast to pregnancy, we observed no significant accumulation of all the subsets of T cells examined at 60 dpi (Supplemental Figs. S4 and S5).

DISCUSSION

We previously showed that IAV infection during pregnancy results in endothelial dysfunction of the aorta and was attributed to IAV disseminating into the thoracic aorta, prompting an innate and adaptive T-cell response, termed "the vascular storm" (7). In the current study, we demonstrated that IAV infection during pregnancy induces the chronic accumulation of various subsets of T cells in the aorta, long after viral clearance and disease resolution in the lungs. This was in striking contrast to nonpregnant mice infected with IAV where there was no evidence of T-cell accumulation within the aorta. The general phenotype of T cells accumulating within the aorta following gestational IAV infection were $CD4^+$ and $CD8^+$ T cells, with a substantial population of IAV-specific $CD8^+$ T cells. When the T-cell subsets were assessed, significant increases were observed in $CD4^+$ and $CD8^+$ naïve, T_{CM} and T_{EM} cells with T_{EM} cells being the predominant subset. In addition, IAV-specific $CD8^+$ T cells predominantly expressed a T_{EM} phenotype. We also observed significant and sustained increases in $CD4^+$ and $CD8^+$ T cells with a $CD44^{hi}CD69^{hi}$ phenotype, which would include T_{RM} cells. The increase in T-cell populations in the aorta was associated with increased expression of IFN-γ mRNA and long-term endothelial dysfunction.

Figure 1. Vascular endothelial dysfunction persists in pregnant mice post-viral clearance. Vascular function was measured in isolated thoracic aortic rings of pregnant mice infected with PBS or HKx-31(X-31) at 10^4 pfu for assessment at 12, 30, and 60 dpi. *A*: schematic of experimental design and wire myography setup. *B–G*: endothelium-dependent and -independent vasodilation to acetylcholine (ACh) and sodium nitroprusside (SNP) at 12 (*B* and *C*), 30 (*D* and *E*), and 60 (*F* and *G*) dpi. *H*: vascular function was measured in isolated thoracic aortic rings of nonpregnant mice infected with PBS or X-31 at 10^4 pfu for assessment of endothelium-dependent vasodilation to ACh at 60 dpi. Vascular relaxation was calculated as a percentage of preconstriction to thromboxane agonist U-46619. A two-way analysis of variance (ANOVA) followed by Holm–Sidak post hoc multiple comparison was used for statistical analysis, $*P < 0.05$. *I*: systolic blood pressure measurements. *J*: Student's *t* test was used for statistical analysis, $***P < 0.005$ mRNA expression of IFN-γ in the thoracic aorta. Fold change calculations in the X-31 group were measured via qPCR, performed against the PBS group within its respective time point and normalized against RPS18. Mann–Whitney *t* test was used for statistical analysis, $*P < 0.05$. *B–G*: data represent pregnant PBS, $n = 4–7$ animals; pregnant X-31, $n = 4–7$ animals; of at least two independent experiments. *H*: data represent PBS, $n = 6$ animals; X-31, $n = 5$ animals; of at least two independent experiments. Results are presented as means ± SE. pfu, plaque-forming units. Images created with a licensed version of BioRender.com.

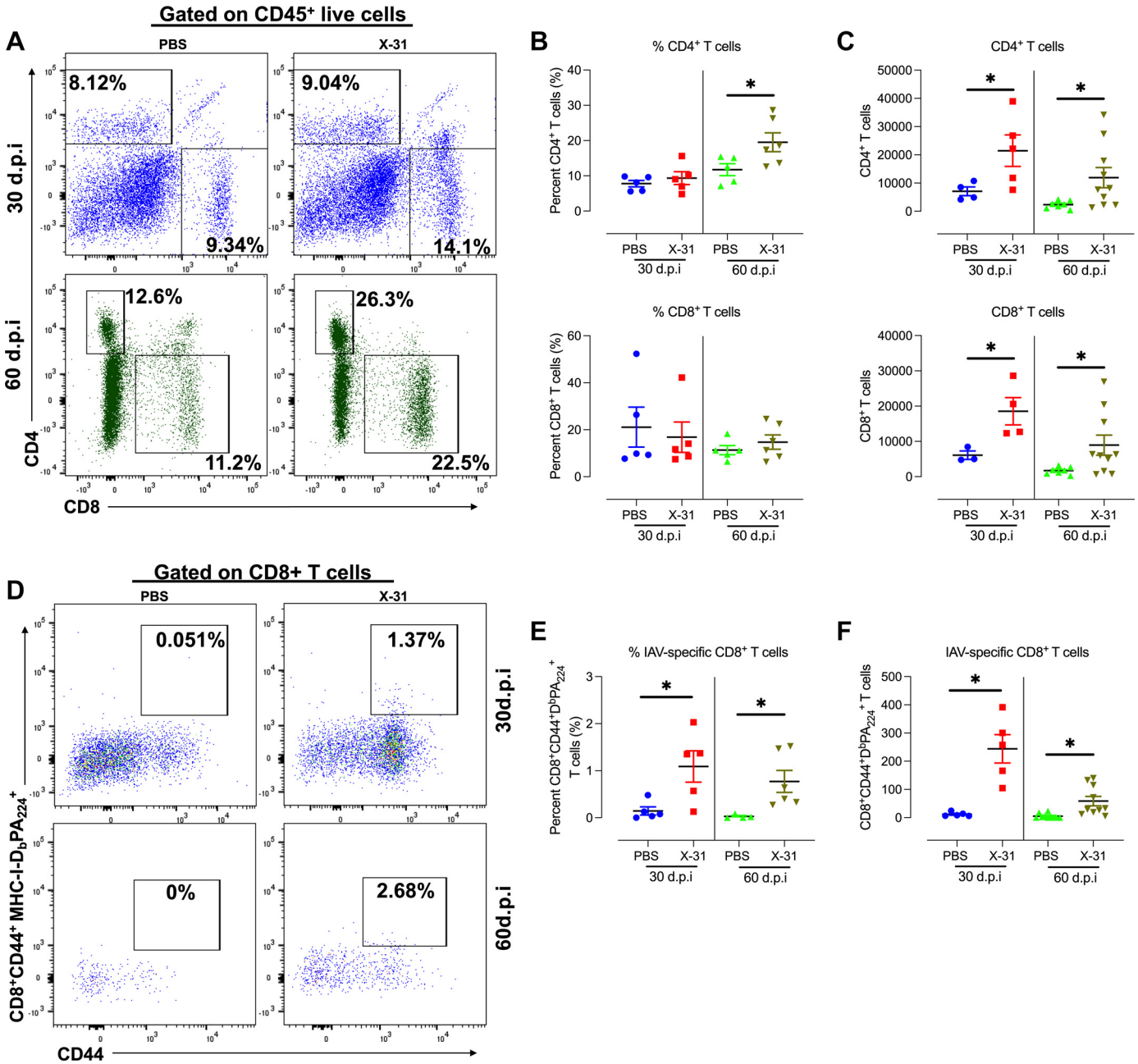

Figure 3. $CD4^+$ and $CD8^+$ T cells are persistently elevated in the aorta post-viral clearance. Pregnant 8–12-wk-old mice were inoculated with PBS or HKx-31 (X-31) at 10^4 pfu. Mice were culled at 30 and 60 dpi, and aorta single cell suspensions were assessed via flow cytometry. *A–C*: representative FACS plots (*A*) and graphs showing the proportion of live $CD45^+$ leukocytes that are $CD4^+$ or $CD8^+$ T cells (*B*) and number of $CD4^+$ and $CD8^+$ T cells (*C*) recovered from aortic tissue. *D–F*: representative FACS plots (*D*) and graphs showing the proportion of $CD8^+$ T cells that are $CD44^+$ and D^bPA_{224} tetramer$^+$ (*E*) and number of $CD8^+$ $CD44^+$ D^bPA_{224} tetramer$^+$ (*F*) T cells. All data shown represent pregnant PBS, $n = 4$–7 animals; pregnant X-31, $n = 4$–10 animals; of at least two independent experiments. All cell populations are measured as the absolute number of cells per 25,000 counting beads. Results are presented as means ± SE. Unpaired Student's *t* test was used for statistical analysis against respective PBS controls. pfu, plaque-forming units. $^*P < 0.05$.

IAV disseminates into the aorta in both pregnant and nonpregnant mice but IAV-induced vascular dysfunction with T-cell inflammation is only seen in pregnant mice. We contend that this vascular pathology owes its origin to the IAV-induced pregnancy-specific vascular storm phenotype, which is characterized by a profound innate and adaptive immune response and oxidative stress (7). We previously reported that endothelial dysfunction in pregnancy occurs as early as 1 dpi and is evident at 3 and 6 dpi (9). Along with a vascular storm, the expression of IFN-γ is likely a major determinant of the vascular pathology, because increased expression of IFN-γ in the vessel wall and PVAT is known to promote VCAM-1 expression to facilitate endothelial cell and VSMC apoptosis (22, 23). The potential for persistent expression of IFN-γ at 30 and 60 dpi may explain why endothelial dysfunction persists after viral clearance and even after newborn delivery. This dysfunctional pathology also shares similarities with the vascular pathology in hypertension (8).

Studies by Guzik et al. (8) in hypertensive mouse models have demonstrated that angiotensin II administration increases vascular effector T-cell populations in the aorta, which in turn leads to IFN-γ production that contributes to vascular dysfunction. Moreover, the low activation threshold of vascular memory T cells favors rapid, nonspecific cytokine secretion (8). Moreover, in atherosclerotic ApoE$^{-/-}$ mouse models, T lymphocytes and macrophages were reported to secrete IFN-γ, which contributes to the pathogenesis of atherosclerosis via the initiation of proatherogenic immune responses (24, 25). Given that memory CD8^{+} T cells can rapidly increase IFN-γ production upon antigenic or cytokine stimulation, it is plausible that reactivated T cells produce high levels of IFN-γ during IAV infection within the aorta and thus promote the persistent endothelial dysfunction. Studies have shown that IFN-γ$^{-/-}$ mice are partially protected against angiotensin II-induced vascular dysfunction, whereas IFN-γ overexpressing mice showed constitutive vascular dysfunction (26). Future studies will be focused on establishing how T cell-derived IFN-γ is driving endothelial dysfunction.

To determine whether endothelial dysfunction was associated with hypertension in our mouse model, blood pressure was measured during pregnancy (6 dpi) and at postpartum (60 dpi). We have previously shown that IAV infection during pregnancy (6 dpi) is associated with endothelial dysfunction (7); however, blood pressure measurements taken in this study found a significant drop in systolic blood pressure in IAV-infected mice. This decrease in systolic blood pressure was transient and returned to uninfected baseline levels by 60 dpi. Despite no change in systolic blood pressure in IAV-infected mice at 60 dpi, future experiments using angiotensin-II infusion would confirm whether resistance vessels from 60-dpi pregnant mice are more susceptible to increased inflammation and endothelial dysfunction compared with uninfected mice. In such studies, we will also measure vascular reactivity using resistance vessels like the mesenteric arteries (27).

We have previously established that IAV disseminates and infects the aorta during pregnancy and involves an exacerbated immune response. In the aorta, there was a significant recruitment of CD69^{+} and CD44^{+} effector T cells, which are known to secrete IFN-γ (8, 16), and this was initiated at 6 dpi during the vascular storm (7). Usually following peak adaptive immune response at ~10 dpi, effector T-cell populations contract, transitioning to long-term memory cells. Post-viral RNA clearance in our study, the CD44^{hi}CD69^{hi} T-cell populations were still present in IAV-infected pregnant mice. It is possible that viral antigenic material remains in the aorta, leading to persistent T-cell activation in the aorta that could drive IFN-γ production and vascular dysfunction. A more likely model is that the expanded CD44^{hi}CD69^{hi} T-cell population represents memory T cells, especially T_{RM} and T_{EM} cells whose reduced activation threshold and rapid capacity for IFN-γ production could trigger the vascular dysfunction phenotype. In hypertension following an adaptive immune response, memory T cells comprising mostly T_{EM} cells accumulate in the aorta and, in the presence of a second or repeated hypertensive stimuli, T_{EM} cells exacerbate hypertension (18, 28). In addition, another potential stimulus for persistent T-cell activation is neoantigen production (formed during prehypertension), which could be produced in response to the oxidative modification of nucleic acids, proteins, or lipids (29). These neoantigens have been proposed to promote hypertension by interacting with antigen-presenting cells to trigger T-cell activation, which in turn initiates a positive feedback loop to facilitate oxidative stress, vascular inflammation, and vascular dysfunction and the formation of more neoantigens (30). Further studies are needed to investigate if the persistent T-cell activation and vascular endothelial dysfunction phenotype observed during IAV infection is partly attributed to neoantigen formation.

Although we observed increased T-cell accumulation in the aorta, it is unclear whether these T cells are migratory or tissue-resident T cells. Further studies are needed to determine whether this increased aortic T-cell pool is derived from the migration of circulatory T cells or the proliferation of tissue-resident aortic T cells. A limitation in this regard is that we did not perform constriction response curves (i.e., phenylephrine) to assess vascular smooth muscle function. We have shown that the vascular smooth muscle response to the vasoconstrictor U46619 is impaired in the aorta at 60 dpi, suggesting that IAV infection in pregnancy may also compromise the integrity of the vascular smooth muscle in the long term. Given the role of smooth muscle cells in the pathogenesis of cardiovascular diseases (31), a more comprehensive assessment of the vascular smooth muscle following IAV infection warrants further investigation. These studies need to incorporate assessments of potential remodeling of the aorta, particularly at the *day 60* time point, which might have also influenced the force responses to U46619, as observed in the current study.

It is widely regarded that IAV infection can cause extensive acute cardiovascular morbidity as well as mortality in patients with underlying cardiovascular disease. This is exemplified by the influenza vaccination being associated with a lower risk of all-cause mortality, cardiovascular mortality, and major adverse cardiovascular events (32). Although IAV can drive acute cardiovascular complications, the findings of the present study ignite new hypotheses that IAV infection is a significant trigger for long-term disease sequelae affecting the cardiovascular system and that pregnancy is a major risk factor for these chronic manifestations. Indeed, this hypothesis is supported by the epidemiology of the cardiovascular disease epidemic of the 1960s that suggests that the high case fatality rates of cardiovascular disease were the delayed result of the 1918 influenza pandemic (33), although a causal role has never been established. The major limitation of these epidemiological studies lies in the difficulty to determine if those who died during the heart disease epidemic were also people who were infected by the Spanish flu and those who were alive during the pandemic but were not infected. Our preclinical study here provides an important clue that IAV infection during pregnancy can lead to long-term endothelial dysfunction and that the accumulation of various subtypes of T cells in the vasculature might play a causative role in triggering future cardiovascular complications in women. Our study also raises significant concerns around the current COVID-19 pandemic and its long-term cardiovascular manifestations in pregnancy. It is conceivable, given that the SARS-CoV2 virus spike protein interacts with ACE2 for cell entry into endothelial cells, that long-term endothelial dysfunction and cardiovascular complications (34) might also arise with this virus. However, it is likely that several decades would need to pass to determine if the COVID-19 pandemic has resulted in a future cardiovascular epidemic. Certainly, in the

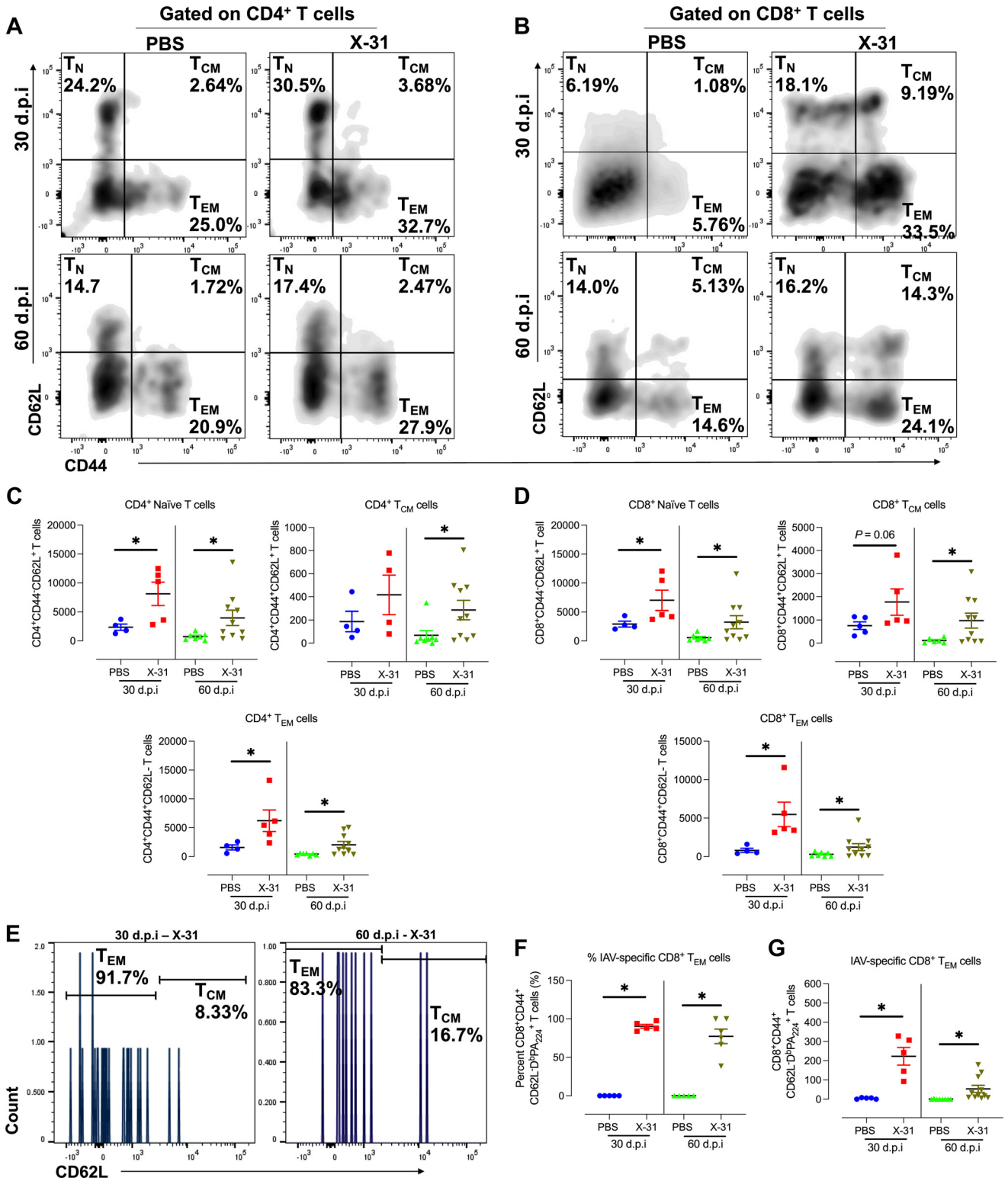

Figure 4. Naïve-, central memory T (T_{CM})-, and effector memory T (T_{EM})-cell subsets within $CD4^+$ and $CD8^+$ T-cell populations in the aorta post-viral clearance. Pregnant 8–12-wk-old mice were infected with PBS or HKx-31 (X-31) at 10^4 pfu and culled at 30 and 60 dpi. Aorta single cell suspensions were assessed via flow cytometry. *A–D*: representative FACS plots for $CD4^+$ (*A*) and $CD8^+$ (*B*) T cells and graphs of numbers of $CD4^+$ (*C*) or CD^{8+} (*D*) naïve ($CD44^-CD62L^+$), T_{CM} ($CD44^+CD62L^+$), and T_{EM} $CD44^+CD62L^-$) cells in the aorta. *E–G*: representative FACS plots (*E*) and graphs showing the proportion of IAV-specific $CD8^+$ that are T_{EM} cells (*F*) and the number of IAV-specific $CD8^+$ T_{EM} cells (*G*) in the aorta. Data shown represent pregnant PBS, $n = 4–7$ animals; pregnant X-31, $n = 4–10$ animals; of at least two independent experiments. All cell populations are measured as the absolute number of cells per 25,000 counting beads. Results are presented as means ± SE. Unpaired Student's unpaired *t* test was used for statistical analysis against respective PBS controls. IAV, influenza A virus. pfu, plaque-forming units. $*P < 0.05$.

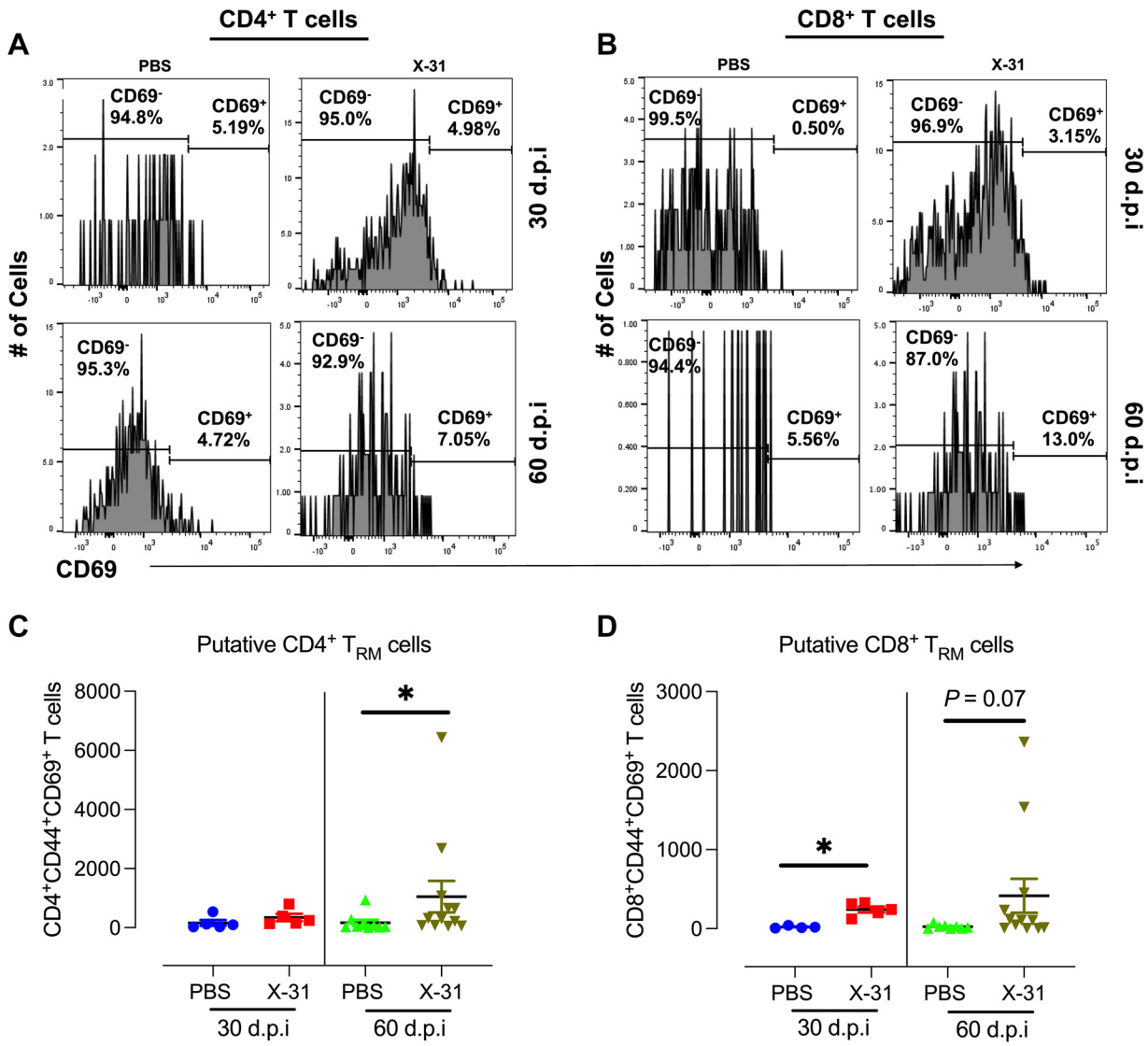

Figure 5. Putative resident memory T (T_{RM}) phenotype cells within $CD4^+$ and $CD8^+$ T-cell populations in the aorta post-viral clearance. Pregnant 8–12-wk-old mice were infected with PBS or HKx-31 (X-31) at 10^4 pfu and culled at 30 and 60 dpi. Aorta single cell suspensions were assessed via flow cytometry. *A–D*: representative FACS plots for putative $CD4^+$ T_{RM} ($CD44^+CD69^+$; *A*) and $CD8^+$ T_{RM} ($CD44^+CD69^+$; *B*) cells and graphs of numbers of putative $CD4^+$ T_{RM} ($CD44^+CD69^+$; *C*) and $CD8^+$ T_{RM} ($CD44^+CD69^+$; *D*) in the aorta. Data shown represent pregnant PBS, $n = 4$–7 animals; pregnant X-31, $n = 4$–10 animals; of at least two independent experiments. All cell populations are measured as the absolute number of cells per 25,000 counting beads. Mann–Whitney *U* test was used for statistical analysis against respective PBS controls. pfu, plaque-forming units. $^*P < 0.05$.

meantime, preclinical animal models will provide strong insight into the chronic cardiovascular effects of IAV, SARS-CoV2, and potentially of other blood-borne RNA viruses.

Cardiovascular disease is one of the leading causes of pregnancy complications and maternal deaths in developed countries. Conversely, pregnancy itself places a significant strain on the cardiovascular system, which may become more amenable to complications or defects when perturbed. The substantial accumulation of T cells together with persistent severe endothelial dysfunction of the aorta following IAV infection in pregnant but not in nonpregnant mice demonstrates that the immunological alterations that occur during pregnancy shape long-lasting changes to the immune profile of the vasculature following prenatal viral infections. These findings present new insight into the role of RNA viruses on acute and chronic cardiovascular complications that are perhaps only revealed with pregnancy. Our study also provides for the first time an important animal model system of cardiovascular complications of pregnancy triggered by common respiratory virus infections such as influenza, advancing our armamentarium of preclinical animal model tools for studying pathophysiology and therapeutic interventions.

A limitation of this study is that we did not assess whether intranasal inoculation per se activates some elements of immune signaling, which could influence the net chronic response to IAV infection. To overcome this, the use of an inactivated virus in future studies would be an ideal control to account for off-target inflammatory effects from the delivery approach and to determine whether IAV-induced chronic vascular dysfunction and T-cell retention in the aorta requires viral replication (35, 36).

In conclusion, IAV infection in pregnant mice leads to long-term endothelial dysfunction of the aorta after viral clearance in the lung and in the aorta. This "long influenza" phenotype associates with elevated IFN-γ mRNA levels in the tissue and persistent retention of a range of T-cell subsets, including $CD4^+$ and $CD8^+$ naïve, T_{CM} and T_{EM} cells, IAV-specific $CD8^+$ T cells, and $CD4^+$ and $CD8^+$ $CD44^{hi}CD69^{hi}$ cells that could include T_{RM} cells. Of note, T_{EM} and T_{RM} cells have been shown in other works to be particularly robust and rapid producers of IFN-γ, making them prime candidates for propagating long-term vascular endothelial dysfunction.

DATA AVAILABILITY

Data will be made available upon reasonable request.

SUPPLEMENTAL MATERIAL

Supplemental Figs. S1–S6: https://doi.org/10.25439/rmt.26156272.

GRANTS

This work was supported by National Health and Medical Research Council of Australia Project I.D. 1122506, 1128276, and 2002948 (to S.S., S.L., R.V., D.A.B., and J.J.O.).

DISCLAIMERS

The funders had no role in study design, data collection and analysis, decision to publish, or preparation of the manuscript.

DISCLOSURES

No conflicts of interest, financial or otherwise, are declared by the authors.

AUTHOR CONTRIBUTIONS

O.O., K.M.Q., J.J.O., D.A.B., S.L., and S.S. conceived and designed research; O.O., K.M.Q., M.C.S., F.L., M.A.M., and S.L. performed experiments; O.O., K.M.Q., M.A.M., S.L., and S.S. analyzed data; O.O., K.M.Q., M.C.S., M.A.M., R.D.B., R.V., J.J.O., D.A.B., S.L., and S.S. interpreted results of experiments; O.O., S.L., and S.S. prepared figures; O.O., K.M.Q., S.L., and S.S. drafted manuscript; O.O., K.M.Q., M.C.S., F.L., M.A.M., R.D.B., R.V., J.J.O., D.A.B., S.L., and S.S. edited and revised manuscript; O.O., K.M.Q., M.C.S., F.L., M.A.M., R.D.B., R.V., J.J.O., D.A.B., S.L., and S.S. approved final version of manuscript.

REFERENCES

1. **Rasmussen SA**, **Jamieson DJ**, **Uyeki TM.** Effects of influenza on pregnant women and infants. *Am J Obstet Gynecol* 207: S3–S8, 2012. doi:10.1016/j.ajog.2012.06.068.
2. **Neuzil KM**, **Reed GW**, **Mitchel EF**, **Simonsen L**, **Griffin MR.** Impact of influenza on acute cardiopulmonary hospitalizations in pregnant women. *Am J Epidemiol* 148: 1094–1102, 1998. doi:10.1093/oxfordjournals.aje.a009587.
3. **Dodds L**, **McNeil SA**, **Fell DB**, **Allen VM**, **Coombs A**, **Scott J**, **MacDonald N.** Impact of influenza exposure on rates of hospital admissions and physician visits because of respiratory illness among pregnant women. *CMAJ* 176: 463–468, 2007. doi:10.1503/cmaj.061435.
4. **Sciscione AC**, **Ivester T**, **Largoza M**, **Manley J**, **Shlossman P**, **Colmorgen GH.** Acute pulmonary edema in pregnancy. *Obstet Gynecol* 101: 511–515, 2003. doi:10.1016/s0029-7844(02)02733-3.
5. **Kraus TA**, **Sperling RS**, **Engel SM**, **Lo Y**, **Kellerman L**, **Singh T**, **Loubeau M**, **Ge Y**, **Garrido JL**, **Rodríguez-García M**, **Moran TM.** Peripheral blood cytokine profiling during pregnancy and post-partum periods. *Am J Reprod Immunol* 64: 411–426, 2010. doi:10.1111/j.1600-0897.2010.00889.x.
6. **Chang J**, **Streitman D.** Physiologic adaptations to pregnancy. *Neurol Clin* 30: 781–789, 2012. doi:10.1016/j.ncl.2012.05.001.
7. **Liong S**, **Oseghale O**, **To EE**, **Brassington K**, **Erlich JR**, **Luong R**, **Liong F**, **Brooks R**, **Martin C**, **O'Toole S**, **Vinh A**, **O'Neill LAJ**, **Bozinovski S**, **Vlahos R**, **Papagianis PC**, **O'Leary JJ**, **Brooks DA**, **Selemidis S.** Influenza A virus causes maternal and fetal pathology via innate and adaptive vascular inflammation in mice. *Proc Natl Acad Sci USA* 117: 24964–24973, 2020. doi:10.1073/pnas.2006905117.
8. **Guzik TJ**, **Hoch NE**, **Brown KA**, **McCann LA**, **Rahman A**, **Dikalov S**, **Goronzy J**, **Weyand C**, **Harrison DG.** Role of the T cell in the genesis of angiotensin II induced hypertension and vascular dysfunction. *J Exp Med* 204: 2449–2460, 2007. doi:10.1084/jem.20070657.
9. **Oseghale O**, **Liong S**, **Coward-Smith M**, **To EE**, **Erlich JR**, **Luong R**, **Liong F**, **Miles M**, **Norouzi S**, **Martin C**, **O'Toole S**, **Brooks RD**, **Bozinovski S**, **Vlahos R**, **O'Leary JJ**, **Brooks DA**, **Selemidis S.** Influenza A virus elicits peri-vascular adipose tissue inflammation and vascular dysfunction of the aorta in pregnant mice. *PLoS Pathog* 18: e1010703, 2022. doi:10.1371/journal.ppat.1010703.
10. **Croft M**, **Bradley LM**, **Swain SL.** Naive vs. memory CD4 T cell response to antigen. Memory cells are less dependent on accessory cell costimulation and can respond to many antigen-presenting cell types including resting B cells. *J Immunol* 152: 2675–2685, 1994.
11. **Swain SL**, **Weinberg AD**, **English M.** CD4+ T cell subsets. Lymphokine secretion of memory cells and of effector cells that develop from precursors in vitro. *J Immunol* 144: 1788–1799, 1990.
12. **Dutton RW**, **Bradley LM**, **Swain SL.** T cell memory. *Annu Rev Immunol* 16: 201–223, 1998. doi:10.1146/annurev.immunol.16.1.201.
13. **Maurice NJ**, **Taber AK**, **Prlic M.** The ugly duckling turned to swan: a change in perception of bystander-activated memory CD8 T cells. *J Immunol* 206: 455–462, 2021. doi:10.4049/jimmunol.2000937.
14. **Bradley LM**, **Duncan DD**, **Tonkonogy S**, **Swain SL.** Characterization of antigen-specific CD4+ effector T cells in vivo: immunization results in a transient population of MEL-14-, CD45RB- helper cells that secretes interleukin 2 (IL-2), IL-3, IL-4, and interferon gamma. *J Exp Med* 174: 547–559, 1991. doi:10.1084/jem.174.3.547.
15. **Christo SN**, **Evrard M**, **Park SL**, **Gandolfo LC**, **Burn TN**, **Fonseca R**, **Newman DM**, **Alexandre YO**, **Collins N**, **Zamudio NM**, **Souza-Fonseca-Guimaraes F**, **Pellicci DG**, **Chisanga D**, **Shi W**, **Bartholin L**, **Belz GT**, **Huntington ND**, **Lucas A**, **Lucas M**, **Mueller SN**, **Heath WR**, **Ginhoux F**, **Speed TP**, **Carbone FR**, **Kallies A**, **Mackay LK.** Discrete tissue microenvironments instruct diversity in resident memory T cell function and plasticity. *Nat Immunol* 22: 1140–1151, 2021. doi:10.1038/s41590-021-01004-1.
16. **MacRitchie N**, **Grassia G**, **Noonan J**, **Cole JE**, **Hughes CE**, **Schroeder J**, **Benson RA**, **Cochain C**, **Zernecke A**, **Guzik TJ**, **Garside P**, **Monaco C**, **Maffia P.** The aorta can act as a site of naive CD4+ T-cell priming. *Cardiovasc Res* 116: 306–316, 2020. doi:10.1093/cvr/cvz102.
17. **Mikolajczyk TP**, **Nosalski R**, **Szczepaniak P**, **Budzyn K**, **Osmenda G**, **Skiba D**, **Sagan A**, **Wu J**, **Vinh A**, **Marvar PJ**, **Guzik B**, **Podolec J**, **Drummond G**, **Lob HE**, **Harrison DG**, **Guzik TJ.** Role of chemokine RANTES in the regulation of perivascular inflammation, T-cell accumulation, and vascular dysfunction in hypertension. *FASEB J* 30: 1987–1999, 2016. doi:10.1096/fj.201500088R.
18. **Xiao L**, **do Carmo LS**, **Foss JD**, **Chen W**, **Harrison DG.** Sympathetic enhancement of memory T-cell homing and hypertension sensitization. *Circ Res* 126: 708–721, 2020. doi:10.1161/CIRCRESAHA.119.314758.
19. **Maguire JJ**, **Wiley KE**, **Kuc RE**, **Stoneman VE**, **Bennett MR**, **Davenport AP.** Endothelin-mediated vasoconstriction in early atherosclerosis is markedly increased in ApoE-/- mouse but prevented by atorvastatin. *Exp Biol Med (Maywood)* 231: 806–812, 2006.
20. **Day EB**, **Charlton KL**, **La Gruta NL**, **Doherty PC**, **Turner SJ.** Effect of MHC class I diversification on influenza epitope-specific CD8+ T cell precursor frequency and subsequent effector function. *J Immunol* 186: 6319–6328, 2011. doi:10.4049/jimmunol.1000883.
21. **La Gruta NL**, **Kedzierska K**, **Pang K**, **Webby R**, **Davenport M**, **Chen W**, **Turner SJ**, **Doherty PC.** A virus-specific CD8+ T cell immunodominance hierarchy determined by antigen dose and precursor frequencies. *Proc Natl Acad Sci USA* 103: 994–999, 2006. doi:10.1073/pnas.0510429103.

22. **Javanmard SH**, **Dana N.** The effect of interferon γ on endothelial cell nitric oxide production and apoptosis. *Adv Biomed Res* 1: 69, 2012. doi:10.4103/2277-9175.102973.
23. **Rosner D**, **Stoneman V**, **Littlewood T**, **McCarthy N**, **Figg N**, **Wang Y**, **Tellides G**, **Bennett M.** Interferon-gamma induces Fas trafficking and sensitization to apoptosis in vascular smooth muscle cells via a PI3K- and Akt-dependent mechanism. *Am J Pathol* 168: 2054–2063, 2006. doi:10.2353/ajpath.2006.050473.
24. **Voloshyna I**, **Littlefield MJ**, **Reiss AB.** Atherosclerosis and interferon-γ: new insights and therapeutic targets. *Trends Cardiovasc Med* 24: 45–51, 2014. doi:10.1016/j.tcm.2013.06.003.
25. **Whitman SC**, **Ravisankar P**, **Daugherty A.** IFN-γ deficiency exerts gender-specific effects on atherogenesis in apolipoprotein E-/- mice. *J Interferon Cytokine Res* 22: 661–670, 2002. doi:10.1089/10799900260100141.
26. **Kossmann S**, **Schwenk M**, **Hausding M**, **Karbach SH**, **Schmidgen MI**, **Brandt M**, **Knorr M**, **Hu H**, **Kröller-Schön S**, **Schönfelder T**, **Grabbe S**, **Oelze M**, **Daiber A**, **Münzel T**, **Becker C**, **Wenzel P.** Angiotensin II-induced vascular dysfunction depends on interferon-γ-driven immune cell recruitment and mutual activation of monocytes and NK-cells. *Arterioscler Thromb Vasc Biol* 33: 1313–1319, 2013. [Erratum in Arterioscler Thromb Vasc Biol 33: e126, 2013]. doi:10.1161/ATVBAHA.113.301437.
27. **Al Ghouleh I**, **Meijles DN**, **Mutchler S**, **Zhang Q**, **Sahoo S**, **Gorelova A**, **Henrich Amaral J**, **Rodriguez AI**, **Mamonova T**, **Song GJ**, **Bisello A**, **Friedman PA**, **Cifuentes-Pagano ME**, **Pagano PJ.** Binding of EBP50 to Nox organizing subunit p47phox is pivotal to cellular reactive species generation and altered vascular phenotype. *Proc Natl Acad Sci USA* 113: E5308–E5317, 2016. doi:10.1073/pnas.1514161113.
28. **Xiao L**, **Kirabo A**, **Wu J**, **Saleh MA**, **Zhu L**, **Wang F**, **Takahashi T**, **Loperena R**, **Foss JD**, **Mernaugh RL**, **Chen W**, **Roberts J 2nd**, **Osborn JW**, **Itani HA**, **Harrison DG.** Renal denervation prevents immune cell activation and renal inflammation in angiotensin II-induced hypertension. *Circ Res* 117: 547–557, 2015. doi:10.1161/CIRCRESAHA.115.306010.
29. **Kirabo A**, **Fontana V**, **de Faria AP**, **Loperena R**, **Galindo CL**, **Wu J**, **Bikineyeva AT**, **Dikalov S**, **Xiao L**, **Chen W**, **Saleh MA**, **Trott DW**, **Itani HA**, **Vinh A**, **Amarnath V**, **Amarnath K**, **Guzik TJ**, **Bernstein KE**, **Shen XZ**, **Shyr Y**, **Chen SC**, **Mernaugh RL**, **Laffer CL**, **Elijovich F**, **Davies SS**, **Moreno H**, **Madhur MS**, **Roberts J 2nd**, **Harrison DG.** DC isoketal-modified proteins activate T cells and promote hypertension. *J Clin Invest* 124: 4642–4656, 2014. doi:10.1172/JCI74084.
30. **Harrison DG**, **Vinh A**, **Lob H**, **Madhur MS.** Role of the adaptive immune system in hypertension. *Curr Opin Pharmacol* 10: 203–207, 2010. doi:10.1016/j.coph.2010.01.006.
31. **Zhuge Y**, **Zhang J**, **Qian F**, **Wen Z**, **Niu C**, **Xu K**, **Ji H**, **Rong X**, **Chu M**, **Jia C.** Role of smooth muscle cells in cardiovascular disease. *Int J Biol Sci* 16: 2741–2751, 2020. doi:10.7150/ijbs.49871.
32. **Yedlapati SH**, **Khan SU**, **Talluri S**, **Lone AN**, **Khan MZ**, **Khan MS**, **Navar AM**, **Gulati M**, **Johnson H**, **Baum S**, **Michos ED.** Effects of influenza vaccine on mortality and cardiovascular outcomes in patients with cardiovascular disease: a systematic review and meta-analysis. *J Am Heart Assoc* 10: e019636, 2021. doi:10.1161/JAHA.120.019636.
33. **Azambuja MI.** Spanish flu and early 20th-century expansion of a coronary heart disease-prone subpopulation. *Tex Heart Inst J* 31: 14–21, 2004.
34. **Giacca M**, **Shah AM.** The pathological maelstrom of COVID-19 and cardiovascular disease. *Nat Cardiovasc Res* 1: 200–210, 2022. doi:10.1038/s44161-022-00029-5.
35. **Li S**, **Zhang Y**, **Guan Z**, **Li H**, **Ye M**, **Chen X**, **Shen J**, **Zhou Y**, **Shi ZL**, **Zhou P**, **Peng K.** SARS-CoV-2 triggers inflammatory responses and cell death through caspase-8 activation. *Signal Transduct Target Ther* 5: 235, 2020. doi:10.1038/s41392-020-00334-0.
36. **To EE**, **Vlahos R**, **Luong R**, **Halls ML**, **Reading PC**, **King PT**, **Chan C**, **Drummond GR**, **Sobey CG**, **Broughton BRS**, **Starkey MR**, **van der Sluis R**, **Lewin SR**, **Bozinovski S**, **O'Neill LAJ**, **Quach T**, **Porter CJH**, **Brooks DA**, **O'Leary JJ**, **Selemidis S.** Endosomal NOX2 oxidase exacerbates virus pathogenicity and is a target for antiviral therapy. *Nat Commun* 8: 69, 2017. doi:10.1038/s41467-017-00057-x.